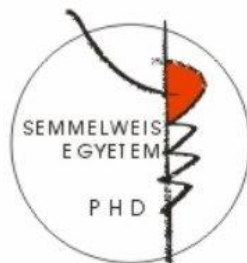


3D ARTIFICIAL MATRICES FOR BIOMEDICAL PURPOSES; SYNTHESIS AND SPECTROSCOPIC CHARACTERISATION

Thesis Booklet

Ákos György Juhász

Semmelweis University
Doctoral School for Theoretical and Translational Medicine



Supervisors:

Angéla Jedlovsky-Hajdú, Ph.D.
László Smeller, DSc.
Abdenacer Idrissi, Ph.D.

Official reviewers:

Sophie Fourmentin, Ph.D.
István Szilágyi, Ph.D.

Head of the Examination Committee:

György Losonczy, DSc.

Members of the Examination Committee:

Andrea Székely, DSc.
Ákos Jobbágy, DSc.

Budapest
2023

1. Introduction

The desire to replace lost body parts has existed since ancient times. Modern advances in biomaterials began in the 1950s and 1960s with the development of synthetic materials like polymers, metals, and ceramics for medical use. Biomaterials continue to evolve with new technologies like 3D printing and materials that mimic natural tissues. Biomaterials are used for medical reconstruction or repair to improve patients' quality of life. Tissue engineering is a rapidly growing field that aims to repair or replace damaged or diseased tissues using a combination of biological and engineering principles. The goal of tissue engineering is to develop functional tissue constructs that can repair or replace lost or damaged tissues in the human body, such as bones, cartilage, blood vessels, and nerves.

Electrospinning technique is one of the method to create micro or nanofiber-based meshes that resemble the extracellular matrix (ECM) of natural tissues. This is important in tissue engineering, where cells are placed on a scaffold that will hold them and could be a base for their structural network like the native ECM. The use of electrospinning in the field of medicine is increasing, as it has the potential to revolutionize the way we create replacement tissues and organs. Conventional electrospinning most of the time faces a limitation notably creating dense fiber structures with small pores which makes it hard for the cells to penetrate. Cotton candy-like three-dimensional structures can be a great alternative which can be achieved by several methods but the most promising is adding salts or nanoparticles. Although there is increasing interest in such structures, the exact cause of their formation has not yet been fully understood. There is a research line of bearing which focusing on the interactions at molecular level to figure out the reason of the fluffy structure formation during electrospinning.

To understand deep molecular level interactions molecular modelling can be used. With the use of computer

simulations one can study the structure and behavior of atomic, and molecular systems. Molecular modelling techniques include molecular dynamics, which simulates the motion of atoms and molecules over time, and quantum mechanics-based methods, which use the principles of quantum mechanics to predict the electronic structure of molecules. These techniques are used in a wide range of fields, including drug design, materials science, and biochemistry.

One of the aim of my thesis was to create reproducibly three dimensional matrices from polysuccinimide (PSI) in the presence of LiCl, CaCl₂ and MgCl₂ salts with the electrospinning technique. PSI is a biodegradable, biocompatible polymer which can be synthesized from aspartic acid. Dimethylformamide (DMF) was used as a solvent.

The other aim of the thesis was to characterize the materials in some of the different stages of the electrospinning process. For this reason first, the interaction of DMF and water (since water vapor is present during the electrospinning process) was characterized from molecular dynamics simulation data with Radial Distribution Function (RDF), Nearest neighbor (NN) and Voronoi polyhedral (VP) methods as the humidity is a key parameter during electrospinning. Then the solvent-salt interaction was characterized with Quantum Chemical calculations and Vibrational Spectroscopy. Lastly, the dry fiber network was characterized with Scanning Electron Microscopy and Vibrational Spectroscopy.

2. Objectives

The main objective of the thesis was the investigation of the 3D scaffold creation of the polysuccinimide based fibrous scaffolds, that can be used later on in tissue engineering. My focus oriented to computational simulation to understand the basic interactions in the solutions and to experimental research covering the creation of the fibers. Thus, my aim was to produce two-dimensional (2D) and three dimensional (3D) poly succinimide based fibrous scaffolds with different salt components, and investigate their interaction with the polymer and the solution.

The objectives of the thesis were the following:

1. To investigate the DMF-water systems with computational simulation to understand the solvent effect in the electrospinning system modelling the humidity. For that MD simulation was performed and analysis was conducted with Radial Distribution Function, Nearest neighbor and Voronoi polyhedra methods
2. To investigate the DMF-salt interaction which can predict the 3D formation during the electrospinning phenomena with DFT calculation and vibrational spectroscopy.
3. To create 3D fibrous scaffold with electrospinning in the presence of different salts for potential tissue engineering applications.

3. Materials and Methods

3.1. Density functional theory (DFT) calculation

The optimized configurations of ions and DMF complexes were obtained in a polar medium treated via an implicit solvent approach. As dispersion plays a vital role in describing the interionic and ions-DMF interactions, the M06-2X functional was used to consider the medium-range dispersion effect better. This functional was coupled with 6-311+g(d,p) basis set.

The geometry optimizations were followed by harmonic frequency analysis to ensure that the obtained structure was true minima by the absence of imaginary wavenumber and to rationalize the experimental results regarding the obtained optimized configurations.

Density functional theory calculations were conducted using Gaussian 16 software package then visualization and analysis were performed with Gaussview 6. The calculations were run on the Zeus cluster of the University of Lille HPC center.

3.2. Molecular Dynamics (MD) calculation analysis

The given MD calculation data of DMF-water (from pure DMF with an increment by 0.1 of water to pure water) were analyzed with Radial Distribution Function (RDF), Nearest Neighbor Contributions (NN), and Voronoi Analysis methods. The RDF and the NN were calculated using TRAVIS-1.14.0 software. All the results of the methods were then curve fitted with Gaussian function and deconvoluted with a python software written by me. The results were then collected and plotted with ORIGIN Pro 9.5.1 software.

The RDF is a function of the distance between pairs of atoms or molecules. It provides information about the probability of finding an atom or molecule at a certain distance from another atom or molecule. The RDF can be used to study the short-range order in a system, such as the arrangements of

atoms in a crystal or the density of molecules in a liquid. It can also be used to study the long-range order in a system, such as the periodicity of a crystal. The RDF can be calculated from various types of simulations.

Nearest neighbor method is used to study the local environment of atoms or molecules in a system. The method involves identifying the closest atoms or molecules to a specific atom or molecule and analyzing their interactions and properties. This approach can give researchers an understanding of the structural, electronic, and thermodynamic characteristics of the system.

Voronoi polyhedra method is a technique that is used to evaluate the local surroundings of atoms or molecules in a system. This method is based on the Voronoi tessellation which partitions space into a set of polyhedral cells, each cell surrounds a specific atom or molecule. The shapes, sizes, and orientations of these polyhedral cells provide information about the coordination of the central atom or molecule and its interactions with its neighbors. This method can be applied to various types of systems, including crystals, liquids, and biomolecules and can be used to evaluate both experimental and computational data to study structural, electronic, and thermodynamic properties of materials. It is particularly useful in identifying defects, impurities, and interfaces in a material and in understanding the behavior of chemical reactions.

3.3. Reagents

L-Aspartic Acid (reagent grade $\geq 98\%$, Mw ~ 133 , Sigma Aldrich, USA), Orthophosphoric Acid (reagent grade $\geq 99\%$, Mw ~ 98 , Sigma Aldrich, USA), N,N-Dimethylformamide (reagent grade $\geq 99.8\%$, AnalaR NORMAPUR®, VWR Chemicals BDH®, VWR International, USA), MgCl_2 ($\geq 99\%$, Reanal), CaCl_2 ($\geq 99\%$, Reanal), LiBr ($\geq 99\%$, Acros Organics), NaBr ($\geq 99\%$, Sigma-Aldrich), NaI ($\geq 99\%$, VWR), KI ($\geq 99\%$, VWR), KBr ($\geq 99\%$, VWR), LiCl ($\geq 99\%$, Sigma-Aldrich).

3.4. Synthesis of Polysuccinimide

Polysuccinimide (PSI) was synthesized with an equipment consists of an IKA RV21 rotary evaporator with an IKA HB21 digital heat tank and a Vacuubrand PC3001 VARIO vacuum generator. The evaporator has a thermostat set to -10 °C and a KOH trap. After carefully mixing 20g L-aspartic acid and 20g crystalline phosphoric acid, the mixture was added to a pear shape flask (1L) and heated to 180 °C under vacuum (3mBar). By the end of a 7-hour-long reaction, one can observe a yellowish-brownish foam-like structure.

When it was cooled down properly, 200 ml dimethylformamide was added and stirred for complete solvation. To remove the unreacted materials, washing and filtering are necessary. 1600ml distilled water was added and stirred for 10 minutes, then with a G3 type glass filter, the mixture was filtered. The washing and filtering steps were repeated about 3-4 times until the pH was neutral. After that, the PSI powder was dried at 40 °C for three days in a dehydrator. The final product had a white color.

3.5. Preparation of solutions

After weighting, the salts were dissolved in DMF stirring on a magnetic stirrer for 8 hours. The polysuccinimide was added to the salt-solvent solution to have a 25 w/w% polymer solution and then further stirred for 12 hours.

3.6. The conductivity of Polymer solutions

The conductivity of the different solutions was measured using a Thermo Scientific Orion 4-Star pH and conductivity meter with a Thermo Orion 013605MD conductivity cell. Calibration points were chosen to have the measured conductivity in between those points. For the measurement, CaCl₂, MgCl₂, LiCl, LiBr, NaBr, NaI, and KI were dissolved in DMF at 1, 3, and 5 w/w% concentrations.

3.7. Electrospinning setup

The electrospinning apparatus consisted of a Genvolt 73030P power supply, a KD Scientific KDS100 pump, a Fortuna Optima 7.140-33 type syringe, and a Hamilton G18 blunt-end steel needle. The collector was a 3D-printed disc of 2 cm diameter, and the distance between the needle and the collector was kept at 10 cm in all cases.

Throughout the electrospinning process, the needle was connected to the positive plug of the power supply, and the ground plug was connected to the collector. When the voltage was applied instantly, a small drop of the polymer was pumped out from the needle to start the electrospinning. The flow rate was set to 1 mL/h, the volume of the polymer solution was 1ml, and the applied voltage was 15 kV in all cases.

3.8. Scanning Electron Microscope (SEM)

From the nanofiber mesh samples, pictures were recorded with a JEOL JSM 6380LA SEM device in the Polymer Technology Department of the Mechanical Engineering Faculty of Budapest University of Technology and Economics. The golden coating was applied to the sample with a JEOL JFC-1200 Sputter Coating System. The accelerating voltage was 10 kV, and the magnification was chosen to be 1000x, 2500x, and 5000x. After electrospinning, samples were collected from three different areas to record pictures from.

The average fiber diameter was analyzed with the Fiji program, and at least 100 fiber diameters were measured from each area at the same magnification. To avoid charge accumulation, silver colloid paint was applied on the edges of the sample. Two-sample Student t-tests were conducted using the averages and standard deviations of the samples to compare the averages double-sided. It was assumed that the fiber diameter showed a normal distribution.

3.9. Fourier transform infrared spectroscopy (FTIR)

FTIR method is primarily used for qualitative measurements. The ATR-FTIR spectra were recorded on the fiber meshes using a JASCO 4700A (JASCO Ltd., ATR Pro ONE) instrument, and the evaluation was performed using the SpectraAnalysis program.

128 parallel measurements were performed for each sample, averaged over the spectra obtained. The spectra of the pure diamond crystal and the saturated water vapor were subtracted from the spectra of the samples. In all cases, the wavenumber detection range was 4000 and 400 cm^{-1} with a resolution of 2cm^{-1} .

ATR-FTIR spectra of the different salt solutions were recorded on a BRUKER Vertex 70V FT-IR instrument. The spectra were acquired, and the baseline was corrected using OPUS 7.5 software and evaluated using Spectragryph 1.2.10 software. For each sample, 64 measurements were performed, detecting between 5000 and 600 cm^{-1} with a resolution of 2cm^{-1} . Deconvolution of the spectra was carried out with Microsoft Excel and its built-in Solver plugin. Gaussian curves were fitted for the peaks and Lorentzian where shoulders appeared.

3.10. FT-Raman spectroscopy

FT Raman spectrometry is a complementary spectroscopic method of infrared spectroscopy. Both investigate the molecular motions of matter, but the sensitivity of each method is different for specific functional groups.

The measurements were performed with a Bruker RFS 100/S FT-Raman instrument. Before the measurement, the detector was cooled with liquid nitrogen and allowed to stabilize for 1 hour. The powdered samples (PSI, LiCl, MgCl_2 , and CaCl_2 powders) and polymer meshes were compressed in a sample holder of a measuring cell before the measurement. The laser beam was focused on the sample surface to achieve maximum intensity, and the laser power was chosen to be

50mW. The resolution was 2 cm^{-1} , and the recorded range was $100\text{-}4000\text{ cm}^{-1}$. To optimize the signal-to-noise ratio, samples were generally measured in 14000 to 22000 replicates. Measurements and baseline correction were performed using OPUS 6.5 software, and evaluations were performed using Spectragryph 1.2.10 software.

4. Results

T1. The local structure of DMF-water mixtures of various concentrations were investigated with Radial Distribution Function (Figure 4.1), Nearest Neighbor and Voronoi polyhedral methods from Molecular dynamics simulation. The results show that while there's a tendency of self-association, generally the two component mix well on the molecular scale. Water-water clusters of no more than 3 and 2 molecules disappearing around DMF mole fraction values of 0.7 and 0.9 respectively. Additionally, DMF molecules form weak, C-H...O type hydrogen bonds with each other in their neat liquid but upon addition of water, these weak H-bonds gradually disappear, because the water molecules can form considerably stronger, O-H...O type hydrogen bonds with the DMF oxygens. [JAGy1]

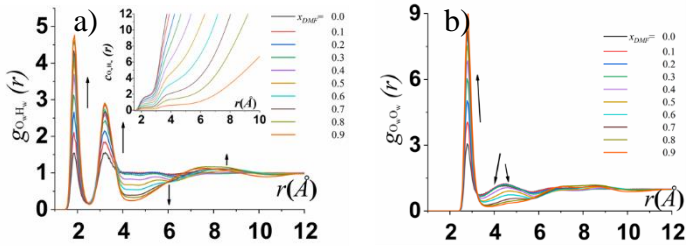


Figure 4.1 Radial distribution function of (a) the water O and H atoms and (b) water O atoms. The arrows indicate the evolution of these functions with increasing DMF mole fraction. The inset shows the running coordination number of the Hw around the Ow atoms in these systems

T2. DMF-salt interactions were characterized with DFT calculations (Table 1 and Figure 4.2). The interatomic distances and frequencies of the C=O, C-H, and $\text{N}^{\text{C}}\text{H}=\text{O}$ modes were specified. The analysis of the distances suggest that the cation is closer to the O atom than the anion, while the anion is closer to the N atom of the DMF than the cation. Generally, the ion-

solvent interaction is responsible for the observed shifts but in the case of C=O vibrational mode it's also orientation of the cation. In the case of C-H bending mode it's also the distance of the anion from H atom, and lastly with the NC^H=O bending mode it's also the distance between the ions and the O and H atoms. The results show that the intermolecular interaction strength with DMF of the salts increase in the following order LiCl < CaCl₂ < MgCl₂. [JAGy2]

Table 1 Intramolecular inter ions and atoms of DMF as obtained by DFT calculations on the configurations

Intra molecular												
	max d(C=O) / Å	min d(C=O) / Å	max d(C-N) / Å	min d(C- N) / Å	max d(C-H) / Å	min d(C- H) / Å	max ((ν) (C=O) / cm-1)	min ((ν) (C=O) / cm-1)	max (δ(C-H)) / cm-1	min (δ(C-H)) / cm-1)	max (δ(NC [^] H=O)) / cm-1)	min (δ(NC [^] H=O)) / cm-1)
4DMF-	1.222	1.216	1.353	1.349	1.104	1.1	1782	1753	1439	1426	678	670
4DMF- 2LiCl	1.228	1.227	1.336	1.336	1.102	1.099	1765	1751	1432	1430	684	681
4DMF- 2CaCl ₂	1.238	1.236	1.329	1.324	1.097	1.097	1747	1733	1428	1427	688	683
4DMF- 2MgCl ₂	1.243	1.231	1.336	1.321	1.096	1.095	1753	1729	1427	1422	705	689

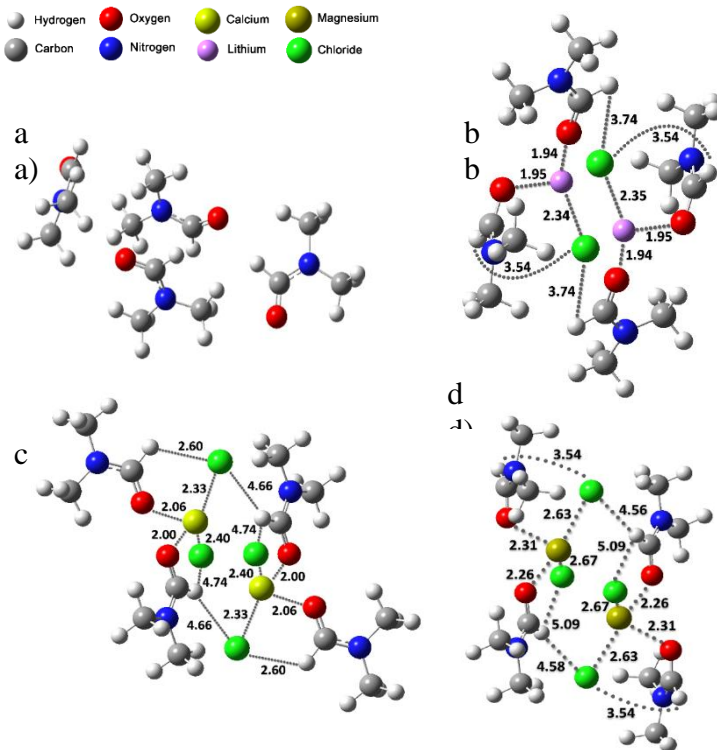


Figure 4.2 Optimized geometries for a) 4DMF b) 4DMF - 2LiCl c) 4DMF - 2CaCl₂ d) 4DMF - 2MgCl₂. Observed interatomic distances (Å) represented with dotted lines.

T3. DMF-salt interactions were characterized with vibrational spectroscopy (Figure 4.3). The results show that the intense C=O vibrational is asymmetric and skewed negatively (~1640 cm⁻¹), due to coordination with Li⁺, Ca²⁺ or Mg²⁺. Another characteristic peak of DMF N^H=O bending peak (660 cm⁻¹) shows a new peak formation very close at 675 cm⁻¹, which can be explained by the complex forming between solvent-salt and salt-salt molecules. The MgCl₂ salt-DMF

mixture exhibits a large upshift in binding strength between the DMF molecules and the ions, indicating that the nature of the salt can influence the strength of these interactions. The data suggests that there are more DMF molecules forming complexes with Li^+ cations than with Ca^{2+} and Mg^{2+} cations, indicating that both the proximity of the DMF molecules to the cation and the nature of the cation can play a role in complex formation. [JAGy2]

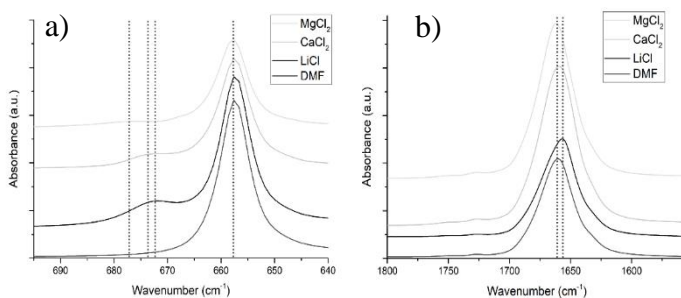


Figure 4.3 IR spectra of the $\text{NCH}=\text{O}$ a) and the $\text{C}=\text{O}$ b) vibrational modes in mixtures of LiCl , CaCl_2 and MgCl_2 2 w/w% with DMF

T4. 3D PSI meshes were electrospun (Figure 4.4.) reproducibly, and characterized with SEM (Figure 4.5) and Vibrational spectroscopy in the presence of CaCl_2 , MgCl_2 and LiCl . The results from FTIR and FT-RAMAN show that there is no chemical change in the end of the electrospinning process, and there's no sign of DMF therefore the fiber meshes are solvent free. The SEM results shows an increase in fiber diameter in the case of CaCl_2 (1w/w%: $660 \pm 220 \text{nm}$; 2w/w%: $675 \pm 110 \text{nm}$; 3w/w%: $950 \pm 150 \text{nm}$) and LiCl (1w/w%: 570 ± 160 ; 2w/w%: 615 ± 100), in the case of MgCl_2 (1w/w%: 470 ± 130 ; 2w/w%: 1230 ± 200 ; 3w/w%: 625 ± 110) it varies greatly, and from the statistical analysis it seems that there's no correlation with the salt concentration and the fiber diameter. CaCl_2 is found to be the best candidate to use since it's

biocompatible and gelation was not observed during preparation resulting better macroscopic 3D structures. [JAGy2]

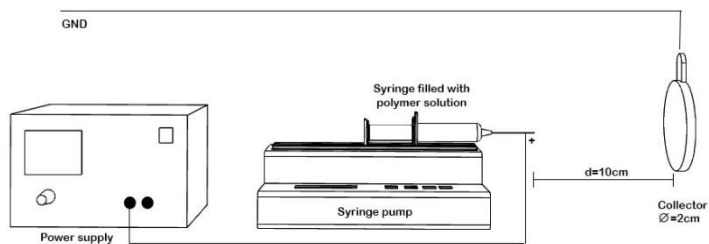


Figure 4.4 Electrospinning apparatus

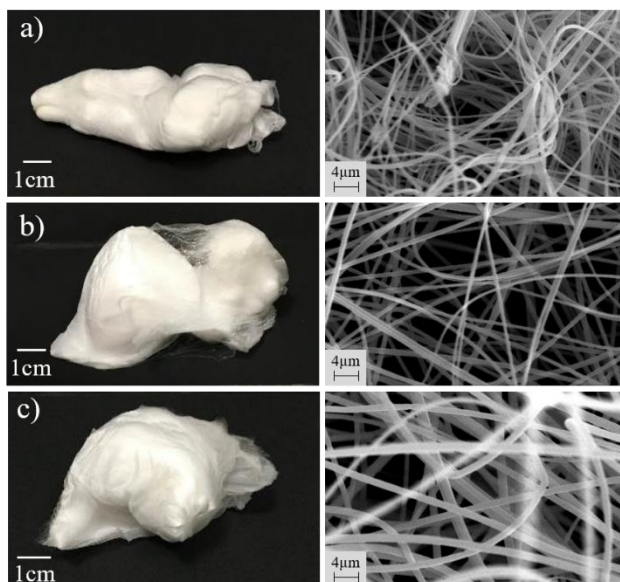


Figure 4.5 Macroscopic picture of the 3D effect of different salts used and their SEM pictures on the right a) LiCl 1 w/w% b) MgCl_2 1 w/w% c) CaCl_2 2 w/w%

5. Conclusion

3D scaffold produced by electrospinning mimic the native extracellular matrix, has better processability than conventional electrospinning. For tissue engineering applications would be ideal to use these scaffolds although the causes of this phenomena are still uncovered. Therefore, my aim was to create and characterize 3D electrospun fibers with electrospinning technique and investigate the behavior of the solvent salt and solvent-water interactions with different computational simulation methods.

Firstly, I analyzed DMF-water mixtures of various compositions from the molecular dynamics simulation data with radial distribution, nearest neighbor and Voronoi polyhedral methods. The results clearly show that DMF mix very well with water on molecular scale, while there's some tendency for self-association even in their dilute systems. The water-water H-bonds are remains while increasing DMF mole fraction values parallel the water clusters are disappearing. This is explained by the increasing CH_3 groups enhance H-bonding structure, and also by the DMF's O atoms can easily replace water oxygens.

Then, I characterized the DMF-salt interactions with DFT calculations and Vibrational spectroscopy. Unlike before, the anion was also included to the calculation. While the concentration of the salt in DMF was quite saturated, the results are align with experimental data. Both the calculated and the experimental data suggest that MgCl_2 tends to have the strongest interaction with DMF (and also water) molecules, while all of them forms complexes with the solvent molecule. Only the salts where complex forming can be found produced 3D structure during electrospinning method, therefore the quality of the salt and its interaction with the solvent molecule is a key to a successful outcome, not just charge accumulation as thought before.

Lastly, I reproducibly created solvent free 3D PSI meshes and characterized with SEM and Vibrational spectroscopy. While one can observe a difference in fiber diameter, from the statistics, there's no correlation with the salt concentration. While gelation occurs at some cases, CaCl_2 can be a good candidate in the future to optimize the electrospinning parameters better and be used for biomedical applications.

These findings can lead to the final understanding how the 3D structure can be achieved with different polymers however, there's still a lot of work ahead

6. Bibliography of the candidate's publications

Publications relevant to the Thesis

[JAGy1]Koverga, Volodymyr ; Juhász, Ákos ; Dudarev, Dmytro ; Lebedev, Maxim ; Idrissi, Abdenacer ; Jedlovszky, Pál: Local Structure of DMF–Water Mixtures, as Seen from Computer Simulations and Voronoi Analysis, JOURNAL OF PHYSICAL CHEMISTRY B 126 : 36 pp. 6964-6978. , 15 p. (2022)

[JAGy2]Juhász, Ákos György; Molnar, Kristof ; Idrissi, Abdenacer ; Jedlovszky-Hajdu, Angela: Salt induced fluffy structured electrospun fibrous matrix, JOURNAL OF MOLECULAR LIQUIDS 312 Paper: 113478 , 10 p. (2020)

Publications not relevant to the Thesis

1. Tóth, Krisztina ; S Nagy, Krisztina ; Güler, Zeliha ; Juhász, Ákos György ; Pállinger, Éva ; Varga, Gábor ; Sarac, A Sezai ; Zrínyi, Miklós ; Jedlovszky-Hajdú, Angéla ; Juriga, Dávid: Characterization of Electrospun Polysuccinimide-dopamine Conjugates and Effect on Cell Viability and Uptake, MACROMOLECULAR BIOSCIENCE in press Paper: e2200397 , 16 p. (2023)

2. Sipos, Evelin ; Juhasz, Akos ; Zrinyi, Miklos: Characteristic load-elongation behavior of weak electrospun fiber texture, JOURNAL OF MOLECULAR LIQUIDS 329 Paper: 115459 , 11 p. (2021)

3. Koverga, Volodymyr ; Maity, Nishith ; Miannay, Francois Alexandre ; Kalugin, Oleg N. ; Juhasz, Akos ; Swiatek, Adam ; Polok, Kamil ; Takamuku, Toshiyuki ; Jedlovszky, Pal ; Idrissi, Abdenacer: Voronoi Polyhedra as a Tool for the Characterization of Inhomogeneous Distribution in 1-Butyl-3-methylimidazolium

Cation-Based Ionic Liquids, JOURNAL OF PHYSICAL CHEMISTRY B 124 : 46 pp. 10419-10434. , 16 p. (2020)

4. Hegedűs, Orsolya ; Juriga, Dávid ; Sipos, Evelin ; Voniatis, Constantinos ; Juhász, Ákos ; Idrissi, Abdenaccer ; Zrínyi, Miklós ; Varga, Gábor ; Jedlovszky-Hajdú, Angéla ; S. Nagy, Krisztina: Free thiol groups on poly(aspartamide) based hydrogels facilitate tooth-derived progenitor cell proliferation and differentiation, PLOS ONE 14 : 12 Paper: e0226363 , 20 p. (2019)